Performance Evaluation of an Optoelectronic Oscillator

Stefania Römisch, John Kitching, Eva Ferrè-Pikal, Leo Hollberg, and Fred L. Walls, *Senior Member, IEEE*

***Abstract*—Phase noise measurements of an optoelectronic oscillator (OEO) at frequencies less than 10 Hz from the carrier (10.6 GHz) as well as the measured Allan variance are presented for the first time. The system has a measured single-side-band (SSB) phase-noise of −123 dB/Hz at 10 kHz from the carrier and a $\sigma_y(\tau) = 10^{-10}$ for an integration time between 1 and 10 seconds. The importance of amplifier phase-noise and environmental fluctuations in determining the noise of the oscillator at these low Fourier frequencies is verified experimentally and analyzed using a generalized model of noise sources in the OEOs. This analysis then allows prediction of the oscillator performance from measured parameters of individual components in the system.**

I. Introduction

TRADITIONAL METHODS used to obtain spectrally pure microwave signals are based on either crystal oscillators (bulk-acoustic wave, BAW, surface acoustic wave, SAW and BVA) or various schemes that utilize high-Q resonators directly in the X-band (like whispering-gallery mode sapphire resonators). In the first case remarkable results have been obtained with BVA oscillators in France [1] with a fractional frequency stability of $6 \cdot 10^{-14}$ at 10 seconds of integration time, but the required frequency multiplication to reach the X-band leads to a degraded spectral purity of the signal. In fact, the phase-noise associated with a 10.6 GHz carrier obtained with noiseless multiplication turns out to be −97 dB_{rad}/Hz[1] at 100 kHz. Our OEO shows −123 dB_{rad}/Hz at 10 kHz from the carrier. In the second case, very low levels of phase-noise spectral density have been obtained, using a room temperature sapphire resonator, in Australia [2] with −150 dB_{rad}/Hz at 1 kHz from the 9 GHz carrier; but data about its stability have not been found, and the resonator requires quite a sophisticated technology.

A feature common to all such oscillators is the small tunability that can be increased only at the expense of stability. An attractive alternative is the idea of the optoelectronic oscillator (OEO) that has been pioneered by X. S. Yao, *et al.* and studied in several laboratories [3]–[5]. These hybrid opto-electronic systems use a long optical fiber as the frequency selective element that permits high tunability and almost no limitation on the range of possible oscillation frequencies, due to the high mode density generated.

It is possible to define, for a fiber in a closed loop, a quality factor similar to the Q factor used for resonators, not based on energetic considerations. In the fiber case, this factor is proportional to the product of the time delay introduced by the fiber and the oscillator's frequency. The important difference with respect to resonator-based oscillators is that, for the OEO, the quality factor is proportional to the oscillation frequency, showing the advantage of having as high a working frequency as possible.

Two undesirable features are the thermal dependence of the fiber length and the non-negligible loss incurred in the conversion from microwave to optical and back again to microwave. To produce oscillation, this loss needs to be compensated, requiring microwave amplifiers that limit the short-term stability due to their flicker phase-noise.

The use of a more general version of the Leeson model, applied to our system [7], allows us to isolate and consider more realistic noise sources than the basic white noise contributions (thermal and optical) previously analyzed in the literature [3], [4]. This analysis then allows the prediction of the oscillator noise performance on the basis of the measured noise of the elements that compose it.

In the next sections, after a brief explanation of the working principle of the oscillator, we describe the OEO prototype realized in our laboratories and present the analysis of the device noise along with related measurements. An evaluation of the features of this kind of oscillator, based on the described analytical and experimental tools, is presented in the last section.

II. The Optoelectronic Oscillator

A. Basic Scheme and Equations

The general configuration for an OEO with external modulation, shown in Fig. 1, includes a CW laser, an electro-optic amplitude modulator (EOM), and a photodetector at the end of the optical fiber. The loop is then closed by an amplification stage, which compensates for loss around the loop, and some kind of filter that selects among the possible modes of this oscillator.

In our system the EOM is a Mach-Zehnder type amplitude modulator, thus,

$$P_{out}(t) = P_{in}(t-\tau_d)\gamma\left[1+\varepsilon\cos\left(\pi\frac{V_{bias}+e_{out}(t-\tau_d)}{V_\pi}\right)\right], \quad (1)$$

Manuscript received July 1, 1999; accepted February 18, 2000.

S. Römisch, J. Kitching, L. Hollberg, and F. L. Walls are with the National Institute of Standard and Technology, 325 Broadway, Boulder, CO 80303 (e-mail: romisch@boulder.nist.gov).

E. Ferrè-Pikal is with the University of Wyoming, Laramie, WY.

[1] 1 dB_{rad} = 1 dB (re to 1 rad^2).

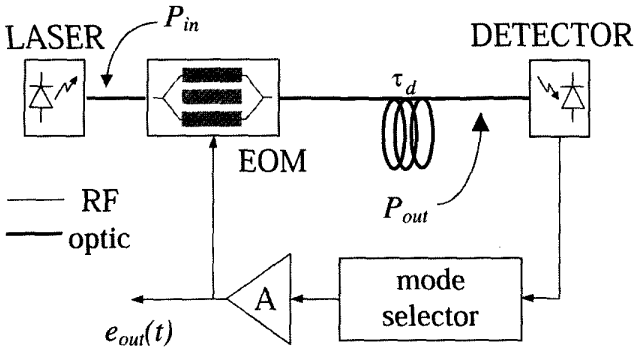

Fig. 1. Basic scheme for an opto-electronic oscillator (OEO) with external modulation.

where P_{in} and P_{out} are the optical powers incident on the modulator and detected at the end of the fiber delay line. The modulator's parameters are γ, the passive insertion loss; ε is a factor related to the extinction ratio, and V_π is the bias voltage needed to move from a maximum to a minimum of the optical power transmittance.

The EOM is biased at the half-transmittance point, so if the RF signal is written as:

$$e_{out}(t) = V_0 \sin(\omega_0 t), \tag{2}$$

the oscillation condition will be set by:

$$P_{in}\gamma\left[1 - 2\varepsilon J_1\left(\frac{V_0\pi}{V_\pi}\right)\sin(\omega_0 t - \omega_0\tau_d)\right] = \frac{V_0}{A\rho}\sin(\omega_0 t), \tag{3}$$

and can be rewritten as:

$$\begin{cases} 2\gamma P_{in}\varepsilon J_1\left(\frac{V_0\pi}{V_\pi}\right) = \frac{V_0}{A\rho}, \\ \omega_0 = \dfrac{(2K+1)\pi}{\tau_d}, \qquad K = 1, 2, 3 \ldots. \end{cases} \tag{4}$$

where A is the gain of the RF amplifiers, ρ includes the detector responsivity and the fiber coupling loss, and $\omega_0 = 2\pi\nu_0$ is the oscillation angular frequency. The total delay along the loop is assumed to be the fiber delay τ_d, neglecting the much smaller delays of the other elements of the system. The mode selector in Fig. 1 selects a particular value of K ($K \cong 33\,455$ in our case) among all the solutions of (4). Both the mode selector as well as the amplifiers are assumed to have a large enough bandwidth that they do not affect the dynamics of the system.

In a more detailed analysis, the mode selector is described by a Lorentzian-shaped transfer function, and the phase delay introduced by the amplifiers also is considered [7]. As a consequence, (4) becomes:

$$\omega_0\tau_d + \Phi_A + 2Q_L\frac{\omega_0 - \omega_R}{\omega_R} = (2K+1)\pi, \quad K = 1, 2, 3 \ldots \tag{5}$$

where Φ_A is the phase delay due to the amplifiers, Q_L is the quality factor of the mode selector and ω_R is its center frequency.

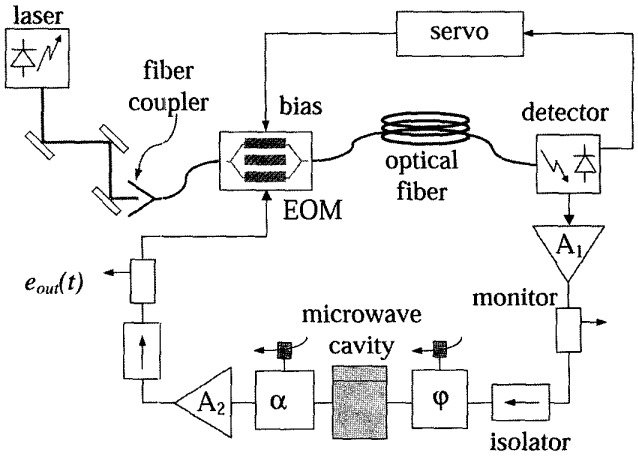

Fig. 2. Experimental setup for the OEO in which the variable attenuator is labeled with α and the variable phase shifter is labeled with φ.

The dependence of the oscillator frequency on system parameters, other than the optical fiber length, is clearly shown in (5). From this it is possible to obtain the expression for the frequency pulling due to the mode selector

$$\omega_0 - \omega_F = \frac{2Q_L}{\omega_R\tau_d + 2Q_L}(\omega_R - \omega_F) \cong \frac{Q_L}{Q_F}(\omega_R - \omega_F), \tag{6}$$

where ω_F is the oscillator frequency if the fiber length alone determined it, and Q_F is the quality factor defined for a fiber as:

$$Q_F = \frac{\omega_0\tau_d}{2}. \tag{7}$$

The OEO, therefore, can be included in the well-known cases of coupled oscillators with different selective elements. In particular, if Q_L, the quality factor of the mode selector, is high, its stability will influence the resulting stability of the oscillator.

B. Experimental Setup

The experimental setup is shown in Fig. 2. The laser is an InGaAsP distributed feedback laser (DFB) with a 3 mA threshold current and a maximum output optical power of 70 mW at a current of 200 mA. In our present experiments, a 100 mA injection current is used with an optical output power of about 35 mW. After passing through an optical isolator, the output beam is coupled into the input fiber of the EOM.

The EOM has an optical insertion loss of about 3 dB and a V_π of about 6 V measured at the operating condition of the oscillator, that is, with a 10.6 GHz signal at the RF port. A servo system is used to keep the bias point of the EOM stable. At this point (after the EOM) the remaining optical power is 7% of the laser output power; the fiber coupling efficiency is 28%, the passive insertion loss of the modulator is 50%, and another 50% is lost due to the half-power bias point of the EOM.

The optical delay between the EOM and the detector is provided by a 1.2 km, single-mode, temperature-compensated optical fiber. This fiber has a temperature dependence of optical delay of 3 ps/(km·K) (compared to the typical fiber coefficient of about 30 ps/km·K)).

The detector is a commercial device with a bandwidth of 25 GHz and an inferred responsivity of 0.17 A/W. Although we are able to obtain the maximum modulation depth, according to (3), with the EOM input RF power near 22 dBm[2], the detected RF signal is only −37 dBm. The total conversion loss from microwave to optical and back to microwave is about 62 dB. The photodetector sees about 1.75 mW of light, corresponding to 5% of the optical power delivered by the laser. These numbers set the minimum gain, which needs to be provided by the RF amplifiers. A low-noise high-gain amplifier provides the first 45 dB of gain, and a low-noise high-power amplifier provides the rest of the required gain and delivers the 22 dBm signal (with some amount of compression) to the RF modulator port.

The mode selector is a critically coupled microwave cavity, which introduces 6 dB of loss. It is placed between the two amplifier stages. The variable attenuator allows us to control the amount of compression in the system. The resulting microwave signal delivered by the oscillator has a RF power of 22 dBm. A side-mode suppression of about 73 dB is due to the filter cavity, which has a loaded quality factor Q_L of about 8300.

III. The Noise

The phase-noise of this oscillator can be predicted using a simple model based on the one described by Leeson [8], which is obtained with the application of control system theory in the Fourier domain [7]. Fig. 3 is a simplified block diagram that represents the OEO in which the block $L(\omega)$ consists of the laser, the EOM, the optical fiber, and the detector. Noise sources represented by $N(\omega)$ are added at the input of each block. The noise spectra present at each summing junction are related to phase-noise spectra by:

$$N(\omega) = V_S \Delta\Phi(\omega) \tag{8}$$

where the V_S is the amplitude in the signal at the summing junction. By applying basic control system theory it is possible to write:

$$\Delta\Phi_{out}(\omega) = \frac{LA_1HA_2\left[\Delta\Phi_1(\omega) + \Delta\Phi_H(\omega) + \Delta\Phi_2(\omega)\right] + \Delta\Phi_L(\omega)}{1 - LA_1HA_2}. \tag{9}$$

In terms of power spectral densities, it then can be written as:

$$S_\varphi(f)\big|_{osc} = \left[\frac{\omega_R}{2\pi f\left(\omega_R\tau_d + 2Q_L\right)}\right]^2 \left[S_\varphi(f)\big|_1 + S_\varphi(f)\big|_H + S_\varphi(f)\big|_2 + S_\varphi(f)\big|_L\right], \tag{10}$$

[2]1 dBm = 1 dB (re 1 mW).

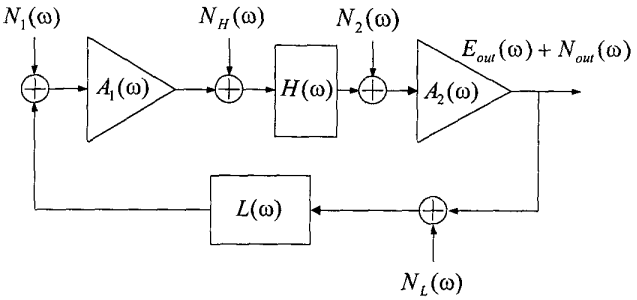

Fig. 3. Block diagram of OEO with main noise sources.

where f is the frequency offset from the carrier, and cross-correlation terms have been neglected. Using this model, we can understand the effects of the different noise sources present in the oscillator.

In previously published analysis of the phase-noise of the OEO, considerable care is dedicated to the thermal and optical generated noise inside the loop, which has a white spectral distribution; but it is not considered, for example, the contribution of the flicker phase-noise of the amplifiers. The white noise sources can provide a faithful description of reality only at frequency offset greater than a few kilohertz from the carrier; but for spectral regions closer to the carrier, as will be clear from the measurements, this is not true anymore. In the original Leeson model [8], the diagram representing the oscillator is composed of only two blocks: a selective element and an amplifier closed in a loop. However, the complete amplifier noise spectra can be included in the model.

In the approach followed in this paper, a model for the oscillator more complicated than the one proposed by Leeson [8] is considered. Moreover, it is possible to insert the measured noise spectra of the single components of the oscillator in (10), verifying experimentally their contribution in the OEO phase-noise.

We start considering the noise contributions of the detection process and the amplification stages. The detection stage equivalent circuit is shown in Fig. 4, with the photodetector simply terminated with a 50 Ω resistor, called R, and I_d being the noiseless photocurrent, containing both a DC and a RF component. At microwave frequencies the detector has two white noise sources, the resistor's thermal noise and the photocurrent shot noise. With an optical power of 1.75 mW incident on the detector with a responsivity of 0.17 A/W, the shot-noise is $\overline{i^2_{shot}} = 2eI_d \cong 10^{-22}$ A^2/Hz, while the thermal noise is $\overline{i^2_{therm}} = 4kT/R \cong 1.4 \cdot 10^{-21}$ A^2/Hz.

Then, the white phase-noise delivered to the load, calculated from the circuit in Fig. 4, will be (see (11) top of next page): where P_{rf} is the signal power measured at the detector output (−37 dBm). Thus at this level of photocurrent, the term associated with the resistor's thermal noise is clearly dominant.

Instead of characterizing each amplifier separately, the equivalent input phase- noise of all the RF components of

$$S_\varphi(f)\big|_{shot} = \frac{\overline{i_{shot}^2} R^2 R_L}{2P_{rf}(R+R_L)^2} \quad \frac{\text{rad}^2}{\text{Hz}} \quad \Rightarrow \quad S_\varphi(f)\big|_{shot} = -145\,\frac{\text{dB}_{\text{rad}}}{\text{Hz}},$$

$$S_\varphi(f)\big|_{therm} = \frac{\overline{i_{therm}^2} R^2 R_L}{2P_{rf}(R+R_L)^2} = \frac{kT}{P_{rf}} \quad \frac{\text{rad}^2}{\text{Hz}} \quad \Rightarrow \quad S_\varphi(f)\big|_{therm} = -140\,\frac{\text{dB}_{\text{rad}}}{\text{Hz}}, \tag{11}$$

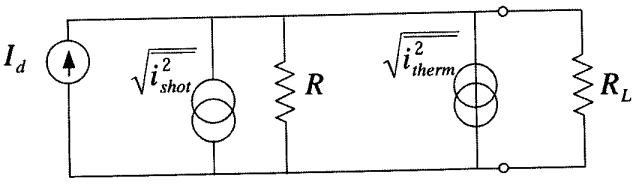

Fig. 4. Photodetector equivalent circuit with shot noise and thermal noise sources. The load resistor is the input impedance of the first amplifier and is assumed to be 50 Ω.

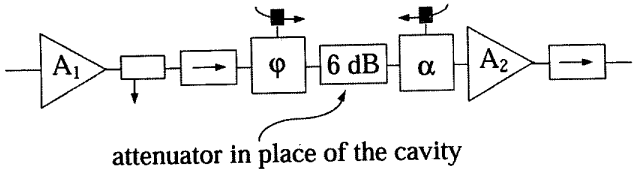

Fig. 5. Block diagram of the ensemble called *RF* chain.

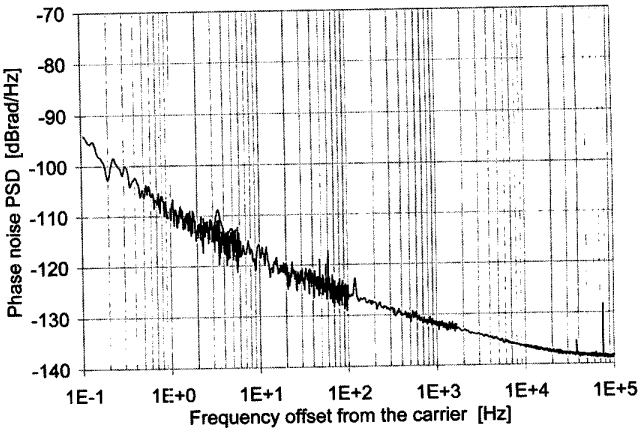

Fig. 6. Phase-noise power spectral density (PSD) of the *RF* chain, measured with a single-mixer homodyne noise-measurement. (*RF* chain input power: −40 dBm, carrier frequency: 10.571 GHz).

the oscillator (except for the cavity) has been measured. The block diagram of this ensemble, called *RF* chain, is displayed in Fig. 5. The measurements have been performed with a single- mixer homodyne noise-measurement system, and the results are plotted in Fig. 6.

The total phase-noise at the input of the RF chain is the sum of the input-equivalent noise of the RF chain and the white noise coming from detection. This resultant quantity can then be substituted into the term $S_\varphi(f)\big|_1$ in (10) to understand the individual contribution of the detection noise and amplifier phase-noise to the total phase-noise of the complete OEO.

The oscillator's phase-noise, plotted in Fig. 7, has been measured with a frequency-discriminator noise-measurement system and can be analyzed in terms of power-law spectral densities. The small portion of white phase-noise (slope f^0) around 100 kHz from the carrier is due to the presence of the adjacent side-mode of the oscillator. For our 1.2 km fiber, the free-spectral range is about 150 kHz, and the side-mode suppression (with the filter cavity) is about 73 dB, comparable with the suppression achieved by Yao *et al.* [9] with the use of two fibers of different lengths.

The next two segments on the phase-noise plot, with slope of 20 dB/decade and 30 dB/decade, respectively, are due to the presence in the oscillator loop of white and flicker phase-noise. In particular, if the measured oscillator's phase-noise is compared with the predicted contributions of the amplifiers and detection process, as shown in

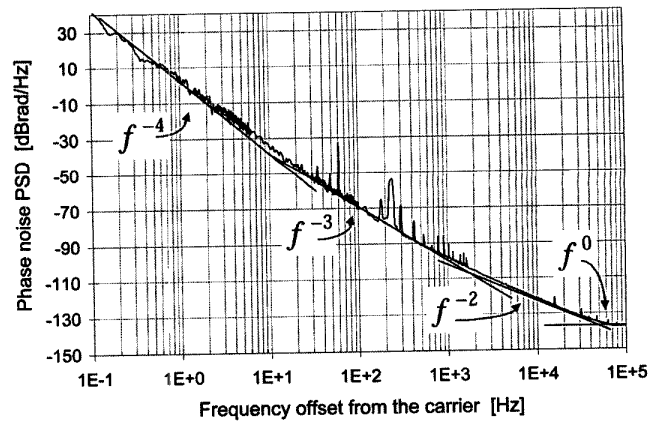

Fig. 7. Measured PSD of the OEO with superposed power law model. The carrier frequency is 10.57 GHz.

Fig. 8, it is clear that the amplifiers play a major role in limiting the spectral purity in this low-frequency portion of the spectrum.

The very low-frequency part of the spectrum shows random-walk frequency noise (slope f^{-4}), and it is known to be related mainly to environmental factors such as temperature fluctuations and vibration. Presumably these could be reduced with proper environmental control, but this was not the objective of the present work [9].

The OEO stability has been characterized in the time domain by two methods: first measuring the frequency relative to a H-maser with a frequency counter, and second

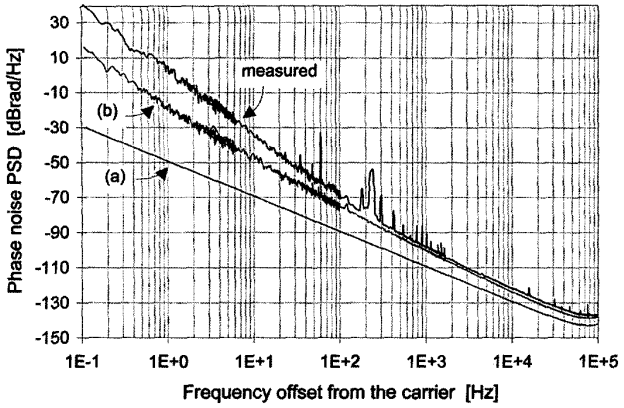

Fig. 8. Measured and predicted phase-noise PSD of the OEO. The noise predictions are made according to the model on the basis of (a) the only white input noise and (b) the total equivalent input noise of the RF section of the loop.

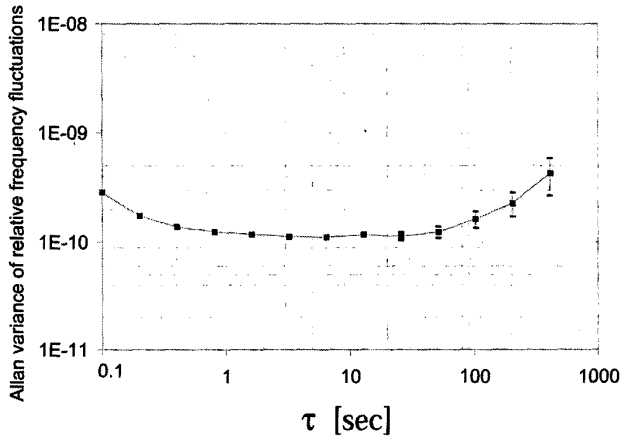

Fig. 9. Measured Allan variance of the relative frequency fluctuations versus integration time τ.

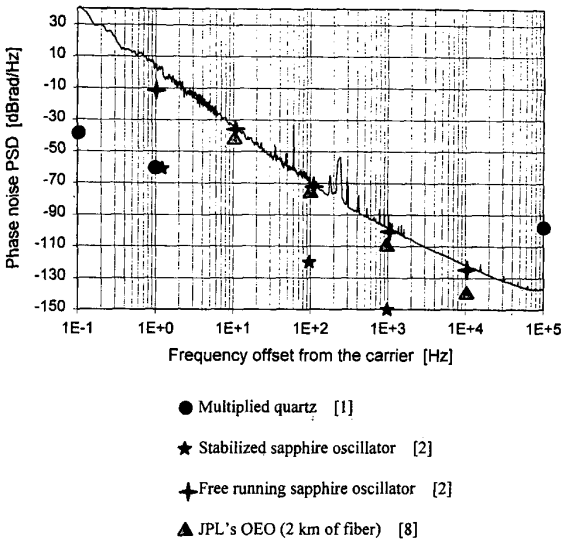

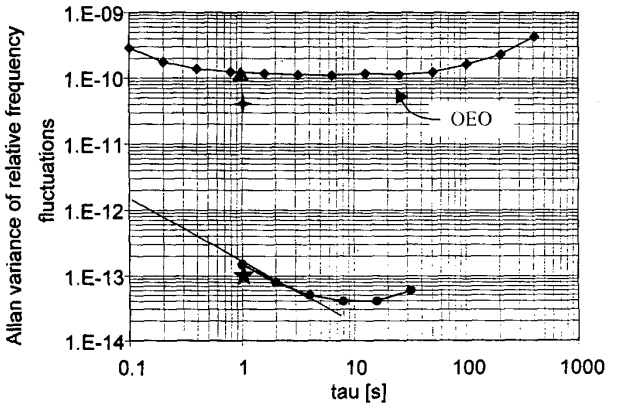

Fig. 10. Comparison between the OEO and the best room temperature oscillators: the French quartz oscillator [1] and the Australian sapphire oscillator [2]. Results achieved by Yao *et al.* for an OEO with a 2 km fiber delay line also are shown [9].

by looking at the fractional frequency fluctuations using the Allan variance. The Allan variance results are shown in Fig. 9: the flat part of the curve is known to be related to the frequency flicker noise of the oscillator (slope f^{-3} in Fig. 8), but the part with slope τ^{+1} is a direct consequence of the thermal drift of the fiber length. Using the asymptotic relations between the Allan variance of the fractional frequency fluctuations and the phase-noise PSD [10], it is possible to obtain:

$$S_\varphi(1\text{ Hz}) = \frac{\sigma_y^2(1\text{ s})\cdot\nu_0^2}{2\ln 2} = 0.81\frac{\text{rad}^2}{\text{Hz}} \Rightarrow -1\frac{\text{dB}_{\text{rad}}}{\text{Hz}}, \quad (12)$$

is a number that confirms the data shown in Fig. 7.

IV. Performance Evaluation

The optoelectronic oscillator has been presented in the introduction as a possible alternative to other, more traditional types of oscillators. Fig. 10 is a comparison, in frequency and time domain, between our unoptimized prototype OEO and the best published examples of quartz oscillator [1] and sapphire oscillator [2] together with the last results of the OEO built by Yao *et al.* [9].

Our results, in terms of phase-noise, are quite good and not too far above the free-running sapphire oscillator. The improvement achieved in the stabilized sapphire oscillator shows that it could be valuable to consider the application of the same technique used by Ivanov *et al.* [2].

The basic idea of their stabilization approach is to use the frequency selective element of the oscillator, that is the fiber for the OEO, as part of a phase-noise discriminator measurement system. The detected noise is then fed back, with the appropriate sign, into the loop of the oscillator reducing the oscillator noise. The noise floor of this measurement system, therefore, represents the limit to the improvement of the oscillator phase-noise performance with this technique. This noise floor depends on the RF

power incident on the selective element and on its coupling efficients. In our OEO, the RF power available for the discriminator can be of the order of -47 dBm ($\cong 20$ μW). This is much less than the power used in the sapphire stabilization scheme. As a result, the projected noise floor in our case would be -118 dB_{rad}/Hz at 1 kHz with a slope f^{-2}, for frequency offsets ranging between 20 Hz and 10 kHz. The only solution to this problem would be to reduce the losses in the microwave-light-microwave conversion. Of the 62 dB mentioned in the description of the experimental setup, optical losses comprise 26 dB. The detection process involves another 12 dB of loss, due to the low responsivity (0.17 A/W) of our high-speed detector. The high RF power required to drive the EOM for significant light modulation causes the remaining 24 dB of losses. The modulator was chosen for an optimized compromise between high bandwidth, low V_π, high optical input power, and, more importantly, commercial availability. Using a detector with a responsivity of 0.7A/W, the noise floor of the discriminator measurement system can be lowered by 6 dB, reaching -124 dB_{rad}/Hz at 1 kHz from the carrier. This leads to a short-term frequency stability of:

$$\sigma_y(\tau) = \sqrt{\frac{S_\varphi(f) f^2}{2\nu_0^2 \tau}} = \frac{4 \cdot 10^{-14}}{\sqrt{\tau}}, \qquad (13)$$

being valid for integration times shorter than one second.

For larger integration times (i.e., smaller offset frequencies for PSD), the noise floor of the system is no longer defined with a slope of f^{-2} [2]. Moreover, the frequency fluctuations due to the fiber length fluctuations become significant, and they cannot be corrected by this noise suppression method because the fiber is part of the measurement system. From (12), it can be seen at the frequency stability between 1 and 10 seconds is determined also by that part of the PSD that has slope f^{-4} (see Fig. 7), that is random walk of frequency, primarily due to environmental fluctuations. As a consequence, the stabilization technique described here will not necessarily lead to a better medium-term stability. To be competitive with the world's best room temperature oscillators, a number of these factors will need to be addressed.

This paper has presented a general and versatile theoretical model for the phase-noise contributions to the OEO noise. In particular, the effect of amplifier phase-noise has been clearly identified and measured.

Experimental data for our OEO prototype, both in frequency domain and time domain, has been provided. In particular, power spectral density of phase noise for frequency offset from the carrier below 10 Hz and Allan variance of the fractional frequency fluctuations have been measured.

A comparison with the best room temperature oscillator available at the moment has been offered with the purpose of putting our OEO, although unoptimized, in a wider context, allowing a better evaluation of the improving factors that need to be addressed.

ACKNOWLEDGMENTS

We thank S. R. Jefferts and F. Ascarrunz for many helpful and illuminating discussions. We also are grateful to R. Mirin and M. Young for carefully reading the manuscript.

REFERENCES

[1] M. Mourey and R. J. Besson, "Performances of new hyperstable BVA oscillators," Workshop on a New Generation of Space Clocks, *Proc. 11th EFTF*, Neuchâtel, 1997.

[2] E. N. Ivanov, M. E. Tobar, and R. A. Woode, "Ultra-low-noise microwave oscillator with advanced phase noise suppression system," *IEEE Microwave Guided Wave Lett.*, vol. 6, no. 9, pp. 312–314, 1996.

[3] X. S. Yao and L. Maleki, "High frequency optical subcarrier generator," *Electron. Lett.*, vol. 30, pp. 1525–1526, 1994.

[4] ——, "Optoelectronic oscillator for photonic system," *IEEE J. Quant. Electron.*, vol. 32, no. 7, pp. 1141–1149, 1996.

[5] J. Kitching, L. Hollberg, and F. L. Walls, "A 1 GHz optical-delay-line oscillator driven by a diode laser," *Proc. IEEE Int. Freq. Contr. Symp.*, 1996, pp. 807–814.

[6] E. N. Ivanov, M. E. Tobar, and R. A. Woode, "Advanced phase noise suppression technique for next generation of ultra low noise microwave oscillator," *Proc. IEEE Int. Freq. Contr. Symp.*, 1995, pp. 314–320.

[7] S. Römisch and A. De Marchi, "Noise predictions for the optoelectronic oscillator using different models," *Proc. IEEE Int. Freq. Contr. Symp.*, 1999, pp. 1100–1104.

[8] D. B. Leeson, "A simple model of feedback oscillator noise spectrum," *Proc. IEEE Lett.*, vol. 54, 1966, pp. 329–330.

[9] X. S. Yao, L. Maleki, Y. Ji, G. Lutes, and M. Tu, "Dual-loop opto-electronic oscillator," *Proc. IEEE Int. Freq. Contr. Symp.*, 1998, pp. 545–549.

[10] J. Rutman, "Characterization of phase and frequency instabilities in precision frequency sources: Fifteen years of progress," *Proc. IEEE*, vol. 66, no. 9, pp. 1048–1075, 1978.

Stefania Römisch was born in Torino, Italy in 1967. She received a degree in electronic engineering in 1993 and a Ph.D. degree in electronic instrumentation in 1998, both from Politecnico di Torino, Italy. Her Ph.D. dissertation work concerned the construction and characterization, both theoretical and experimental, of a class of ultra-stable X-band optoelectronic oscillators, together with the development of a prescaled clock recovery for high bit rate optical time domain multiplexing (OTDM) systems.

In 1994 she was a consultant in the Electronic Department of Politecnico di Torino as well as a guest researcher in the Time and Frequency Division of the National Institute of Standard and Technology (NIST), in Boulder, CO. She is now a guest researcher in the Time and Frequency Division at NIST in Boulder, CO, where she is working on optoelectronic oscillators.

Her research interests are low noise microwave oscillators, analysis of noise processes and noise measurement systems, optoelectronic systems, and frequency metrology.

John Kitching was born in Chester, England, in 1968. He received his B.Sc. degree in physics from McGill University in Montreal, Quebec, Canada, in 1990 and his M.Sc. and Ph.D. degrees in applied physics from the California Institute of Technology in Pasadena, CA, in 1992 and 1995, respectively. His thesis research was on the amplitude and frequency noise properties of semiconductor lasers with optical feedback.

From 1995 until 1998 he was a postdoctoral research associate at JILA and the University of Colorado in Boulder, where he is currently a senior research associate.

His research interests include atomic physics, primary frequency standards, low-noise microwave oscillators, and the applications of semiconductor laser technology to problems in these areas.

Eva S. Ferrè-Pikal received her B.S. degree in electrical engineering from the University of Puerto Rico, Mayaguez, in 1988. In 1989, she received her M.S. degree in electrical engineering from the University of Michigan, Ann Arbor. From 1988 to 1991 she worked for AT&T Bell Laboratories in Westminster, CO. She received her Ph.D. degree from the University of Colorado at Boulder in 1996. The main topic of her thesis was the up-conversion of low frequency noise into amplitude and phase noise in BJT amplifiers.

From 1997 to 1998 she was a National Research Council Postdoctoral Research Associate at the National Institute of Standards and Technology. In 1998 she joined the Electrical Engineering Department at the University of Wyoming as an assistant professor.

Her research interests are phase and amplitude noise processes in oscillators and amplifiers, the generation and synthesis of signals very stable in frequency and amplitude, and the design and applications of low noise devices.

Fred L. Walls (A'93-SM'94) was born in Portland, OR, on October 29, 1940. He received the B.S., M.S., and Ph.D. degrees in Physics from the University of Washington, Seattle, in 1962, 1964, and 1970, respectively. His Ph.D. thesis was on the development of long-term storage and nondestructive detection techniques for electrons stored in Penning traps and the first measurements of the anomalous magnetic (g-2) moment of low energy electrons.

From 1970 to 1973, he was a Postdoctoral Fellow at the Joint Institute for Laboratory Astrophysics in Boulder, CO. This work focused on developing techniques for long-term storage and nondestructive detection of fragile atomic ions stored in Penning traps for low energy collision studies. Since 1973, he has been a staff member of the Time and Frequency Division of the National Institute of Standards and Technology, formerly the National Bureau of Standards in Boulder. He is presently Leader of the Phase Noise Measurement Group and is engaged in research and development of ultra-stable clocks, crystal-controlled oscillators with improved short- and long-term stability, low-noise microwave oscillators, frequency synthesis from RF to infrared, low-noise frequency measurement systems, and accurate phase and amplitude noise metrology. He has published more than 150 scientific papers and articles. He holds five patents for inventions in the fields of frequency standards and metrology.

He received the 1995 European "Time and Frequency" Award from the Societe Francaise des Microtechniques et de Chromometric for "outstanding work in the ion storage physics, design and development of passive hydrogen masers, measurements of phase noise in passive resonators, very low noise electronics and phase noise metrology," He is the recipient of the 1995 IEEE Rabi Award for "major contributions to the characterization of noise and other instabilities of local oscillators and their effects on atomic frequency standards" and the 1999 Edward Bennet Rosa Award for "leadership in development and transfer to industry of state-of-the-art standards and methods for measuring spectral purity in electronic systems," He has also received three silver medals from the US Department of Commerce for fundamental advances in high resolution spectroscopy and frequency standards, the development of passive hydrogen masers and the development and application of state-of-the-art standards and methods for spectral purity measurements in electronic systems. Dr. Walls is a Fellow of the American Physical Society, a Senior Member of the IEEE, a member of the Technical Program Committee of the IEEE Frequency Control Symposium, and a member of the Scientific Committee of the European Time and Frequency Forum.